

The Refolding and Reassembly of *Escherichia Coli* Heat-Labile Enterotoxin B-Subunit: Analysis of Reassembly-Competent and Reassembly-Incompetent Unfolded States[†]

C. Cheesman, L. W. Ruddock,[‡] and R. B. Freedman^{*,§}

Department of Biosciences, University of Kent, Canterbury, Kent CT2 7NJ, U.K.

Received August 21, 2003; Revised Manuscript Received December 8, 2003

ABSTRACT: The B-subunit pentamer of *Escherichia coli* heat-labile enterotoxin (EtxB) is an exceptionally stable protein maintaining its quaternary structure over the pH value range 2.0–11.0. Up to 80% yields of reassembled pentamer can be obtained in vitro from material disassembled for very short incubation periods in KCl–HCl, pH 1.0. However, when the incubation period in acid is extended, the reassembly yield decreases to no more than 20% (Ruddock et al. (1996) *J. Biol. Chem.* 271 19118–19123). Here we demonstrate that the ion species present in the disassembly conditions strongly influence the reassembly competence of EtxB showing that 60% reassembly yields can be achieved, even after prolonged incubations, by the use of a phosphate buffer for acid disassembly. Using this system, we have fully characterized the disassembly and reassembly behavior of EtxB by electrophoretic, immunochemical, and spectroscopic techniques and compared it with that previously observed. Depending on the denaturation system used, the acid-denatured monomer is either in a predominantly reassembly-competent state (H₃PO₄ system) or in a predominantly reassembly-incompetent conformation (KCl–HCl system). Interconversion between these two conformations in the denatured state is possible by the addition of salts to the denatured protein. The results are consistent with the previous hypothesis that the conversion between reassembly-competent and -incompetent states corresponds to a cis/trans isomerization of a peptide bond, presumably that to Pro93.

Escherichia coli heat-labile enterotoxin (Etx), a close relative of cholera toxin and the major causative agent of traveller's diarrhea (1, 2), is a heterohexameric protein comprising one A subunit (EtxA) possessing ADP-ribosyl-transferase activity and five identical noncovalently associated B subunits (EtxB). The B-subunits assemble into a stable pentameric torus that binds to G_{m1} ganglioside receptors found on the surfaces of eukaryotic intestinal epithelial cells even in the absence of the toxic A subunit (2–4). The chemical and biophysical properties of human EtxB (EtxB) have been extensively studied, and the crystal structure has been refined to 1.95 Å resolution (5). Each monomeric B subunit is composed of 103 amino acids and forms approximately 30 hydrogen bonds and six salt bridges with its neighboring subunits to assemble into a highly stable cyclic pentameric structure (6).

In this study, the refolding and pentamer reassembly of the B-subunit have been examined. Each monomeric B subunit contains a single disulfide bond between cysteine residues 9 and 86 and a cis proline residue at position 93 (5). In vitro three rate-limiting steps have been defined on

the refolding pathways of many denatured proteins: disulfide bond formation, trans to cis isomerization of prolyl residues, and oligomerization (reviewed in refs 7, 8). Hence, all of the three “common” intramolecular and intermolecular rate-limiting steps for protein refolding/reassembly are required for EtxB.

Previous in vitro studies have shown that disassembly of the pentamer can be achieved only under extremely harsh denaturation conditions, for example, in the presence of ionic detergents, 8 M urea, or 7 M guanidinium chloride, and in temperatures in excess of 80 °C (9–11). Acid-mediated disassembly of EtxB has only been observed at pH 2.0 and below and is believed to result from protonation of two C terminal carboxylates, which disrupts a salt bridge at the interface between two monomers (10). When the acid incubation period does not exceed 15 s, reassembly yields of up to 80% can be obtained following subsequent neutralization (12). However, when the acid incubation period was extended, a further acid-mediated change occurred that resulted in the generation of assembly-defective species and restricted the reassembly yield to just 20%. This loss of reassembly competence has been attributed to an acid-induced conformational change; its kinetics and activation energy are consistent with it arising from cis/trans isomerization of the cis proline at position 93 (see Figure 1; 12).

Here we show that 60%–65% reassembly yields may consistently be achieved by the use of an alternative acid denaturation system (H₃PO₄). The disassembly process in H₃PO₄ shows differences from that previously reported in

[†] This work was funded by the Biotechnology and Biological Sciences Research Council, Grant Number 96/C 10318.

[‡] Current address: Biocenter Oulu and Department of Biochemistry, P.O. Box 3000, University of Oulu, FIN-90014, Finland.

[§] Current address: Department of Biological Sciences, University of Warwick, Coventry CV4 7AL, U.K. Tel: +44-2476-523516. Fax: +44-2476-523568. E-mail r.b.freedman@warwick.ac.uk.

¹ Abbreviations: Etx, *E. coli* heat-labile enterotoxin; EtxB, B-subunit of *E. coli* heat-labile enterotoxin.

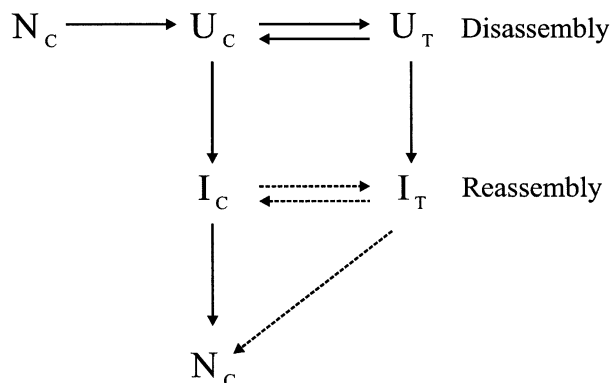


FIGURE 1: Schematic representation of the disassembly and reassembly processes for EtxB. Solid arrows indicate permitted transitions; dashed arrows indicate nonpermitted transitions. Letters represent the unfolded (U), native (N), and nonnative folding intermediate (I) states of the monomeric protein; subscripts represent the cis (C) and trans (T) isomers of proline 93 (adapted from ref 12).

KCl–HCl, and we demonstrate that the structure of the acid-denatured monomer is dependent on the denaturation buffer used. Reassembly studies indicate that the H_3PO_4 system generates a predominantly reassembly-competent state, while the majority of the monomers in the KCl–HCl denaturation system are maintained in a reassembly-defective conformation. Interconversion between these two conformations in the denatured state is possible by the addition of salts to the denatured protein and has the properties of a cis/trans isomerization, suggesting that the prolyl cis/trans equilibrium of acid-denatured EtxB may be manipulated by selective salt effects in denaturing conditions.

EXPERIMENTAL PROCEDURES

Buffers and Solutions. All buffer reagents were purchased from Sigma or Aldrich and prepared in Milli Q purified water. Fresh buffers were prepared daily for disassembly/reassembly studies. All buffers for spectroscopic measurements were filtered through sterile $0.2\ \mu\text{m}$ filters before use. Buffer pHs were determined using a Corning 240 pH meter calibrating at 4.00 and 7.00 with standard buffers supplied by Aldrich. pH calibration was checked using a standard buffer of pH 2.00 supplied by BDH. The pH of H_3PO_4 solutions was adjusted by the addition of NaOH.

Protein Purification. A rifampicin-resistant derivative of marine *Vibrio* sp. 60 (13) was used as a host for the plasmid pMMB68 expressing wild-type EtxB. The bacterial strain was grown, and the recombinant protein was purified by an adaptation of the method previously described (14). Following ultrafiltration, the retentate was buffer-exchanged into 50 mM citrate, pH 5.6, and the protein was bound to a Mono S cation exchange column (Amersham Pharmacia Biotech) and eluted with an increasing linear gradient of 20 mM to 1 M NaCl in this buffer. The peak fractions were diluted 5-fold into 25 mM borate, pH 8.5, containing 20 mM NaCl and concentrated by anion exchange on a Resource Q column (Amersham Pharmacia Biotech). The concentrated samples were buffer-exchanged into borate buffered saline (10 mM borate, pH 8.5, 150 mM NaCl), and the concentrations were determined by spectrophotometric analyses at 280 nm using a calculated molar extinction coefficient of $71\ 500\ \text{M}^{-1}\ \text{cm}^{-1}$ (for the pentamer) and by G_{m1} enzyme-linked immunosorbent

assay (ELISA) as previously described (14). The protein was purified to apparent homogeneity, only a single band being visible on silver-stained SDS–PAGE, with a yield of 8.5 mg/L. The authenticity of the purified protein was confirmed by electrospray mass spectrometry and N-terminal sequencing. Purified protein was stored in $200\ \mu\text{L}$ aliquots at $-20\ ^\circ\text{C}$.

Biophysical Analysis. Amino acid sequencing was performed on an N-terminal protein sequencing Applied Biosystem Procise 492 system. Electrospray mass spectrometry analysis was performed on a Thermoquest LCQ ion trap mass spectrometer.

Protein samples of $2\ \mu\text{g}$ were routinely analyzed using 15% SDS polyacrylamide gels on a Bio-Rad mini Protean II system according to the manufacturer's recommendations, and the separated bands were visualized by staining with 0.05% (w/v) Coomassie blue R250 in 40% (v/v) methanol and 10% (v/v) glacial acetic acid. Pentamers migrate with an M_r of approximately 42 kD and were quantified by densitometric scan of the gels.

Secondary structures were predicted from circular dichroism spectra recorded on a Jasco J600 spectropolarimeter thermostatically controlled at $25\ ^\circ\text{C}$. Far-UV spectra were recorded over the range 190–250 nm in 0.2 nm increments with a cell path length of 0.1 mm. The proteins were diluted in the appropriate buffer. Spectra were acquired at a scan speed of 10 nm/min with a 1 s response time. The spectral data were averaged over four scans, corrected for baseline, and the molar ellipticity values were calculated.

Intrinsic fluorescence was measured on a Perkin-Elmer LS50B spectrofluorimeter. Time-dependent changes in the fluorescence intensity maxima of the proteins (excitation 280 nm, emission 350 nm, slit widths 5 nm) were followed at $20\ ^\circ\text{C}$ using appropriate time drive parameters. Samples were prepared by dilution of protein stock solutions into 1 mL of appropriate pH buffers. pH-dependent conformational changes (pH 3.5–7.0) were recorded at an excitation wavelength of 280 nm, emission of 300–400 nm, and slit widths of 5 nm. Samples were diluted to $12\ \mu\text{g}/\text{mL}$ in appropriate pH buffer (pH 3.5–7.0) and thermally equilibrated at $25\ ^\circ\text{C}$. Emission spectra, corrected for background, were averaged over three scans. All kinetic traces were evaluated using Igor v1.21, Wavemetrics Ltd. In all cases, the time points of the fluorescence spectra have been adjusted to allow for the initial mixing time (typically 15 s).

Disassembly and Reassembly. For disassembly/reassembly studies, protein samples were routinely acid-treated (0.1 M KCl–HCl or 0.1 M H_3PO_4) at a concentration of 1 mg/mL and diluted 10-fold in McIlvaine buffer (0.2 M sodium phosphate, 0.1 M citric acid, usually at pH 7.5 but see text) for renaturation. The reassembly reaction was quenched either by the addition of SDS–PAGE loading buffer or by dilution of the protein to $0.1\ \mu\text{g}/\text{mL}$ in phosphate-buffered saline containing 1% bovine serum albumin. The amount of native pentamers was analyzed by G_{m1} -ELISA and detected by a monoclonal antibody 118.87 (15). In the KCl–HCl disassembly system, 100% pentameric disassembly was observed following 30 min incubation. However, following 2 h incubation in H_3PO_4 a small percentage of EtxB pentamers were consistently observed to remain intact by SDS–PAGE and G_{m1} -ELISA. It appears that disassembly of a small subpopulation of EtxB occurs extremely slowly,

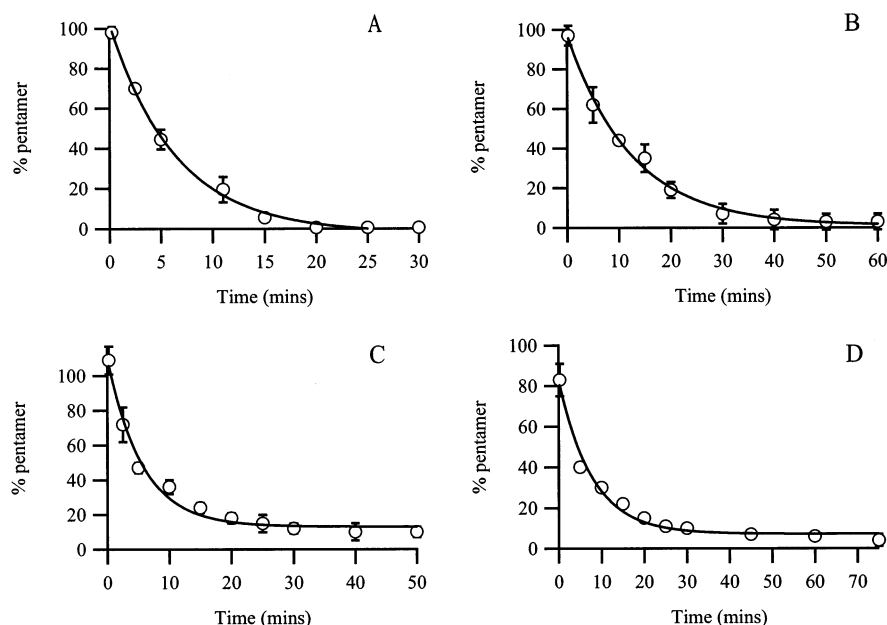


FIGURE 2: Disassembly of EtxB in phosphoric acid: (A, B) time course of disassembly of EtxB in 0.1 M phosphoric acid at ambient temperature as determined by densitometry analyses of polyacrylamide gels ($n = 3$); (C, D) G_{M1} -ELISA analyses ($n = 3$) of the disassembly of EtxB in 0.1 M phosphoric acid at 20 °C. During acid incubation, at time points between 0.25 and 80 min, aliquots were diluted 10-fold into McIlvaine buffer, pH 7.5, followed immediately by a 100-fold dilution into 0.1% BSA in PBS (at this concentration of 1 μ g/mL no reassembly of pentamer occurs): (A) pH 1.7, $k = 0.156 \pm 0.010 \text{ min}^{-1}$ ($r^2 = 0.998$); (B) pH 1.8, $k = 0.081 \pm 0.006 \text{ min}^{-1}$ ($r^2 = 0.994$); (C) pH 1.7, $k = 0.178 \pm 0.021 \text{ min}^{-1}$ ($r^2 = 0.985$); (D) pH 1.8, $k = 0.117 \pm 0.015 \text{ min}^{-1}$ ($r^2 = 0.991$).

and 100% disassembly was only observed when the acid incubation period was extended to 18 h. All reassembly studies were corrected for this small population of un-disassembled material.

RESULTS

Establishment of a Reassembly-Competent Disassembled State for EtxB. In vitro studies of protein folding and assembly must start with the protein in solvent conditions designed to disrupt the noncovalent interactions that stabilize the native conformation. Previous studies on the reassembly of EtxB have used acid denaturation (below pH 2.0) in unbuffered conditions to allow for rapid and effective reversal by neutralization. Specifically, a KCl–HCl denaturation system was used, which allowed for effective unfolding and disassembly of EtxB, but exposure to these conditions beyond a few seconds led to the formation of reassembly-incompetent species (12). Yields of reassembly were maximally 20% except in “double-jump” experiments where yields of up to 80% could be achieved if the protein was disassembled at pH 1.0 for a few seconds and then neutralized. These results were attributed to isomerization of the *cis*-proline at position 93 following denaturation, which could not subsequently be reversed under renaturing conditions.

To study the process of EtxB reassembly in detail and the potential role of protein folding catalysts and chaperones in this process, we sought alternative disassembly conditions that would retain the unfolded subunits in a reassembly-competent state. The very great stability of the pentameric structure restricts possible conditions. We found that, in contrast to the KCl–HCl system previously used, the use of phosphoric acid buffered in the range pH 1.5–2.0 provided well-controlled disassembly conditions from which reassembly yields of around 60% were routinely achieved. Furthermore the yield of reassembly was found to be

essentially independent of the time in acid, up to 18 h; the average reassembly yield after 18 h in disassembly conditions was $59.8\% \pm 4.9\%$ compared with $59.7\% \pm 9.1\%$ after 30 min in disassembly conditions.

Disassembly in Phosphoric Acid. To compare reassembly from the phosphoric acid denatured system with that previously reported for KCl–HCl, we carried out a full characterization of the disassembly process. The initial assays employed were SDS–PAGE, since the native pentamer is resistant to SDS-dissociation, and G_{M1} -ELISA, since only native pentameric EtxB will bind to G_{M1} , so that only pentamers are detected.

EtxB has previously been shown to exhibit a sharp pH threshold for disassembly in 0.1 M KCl–HCl below pH 2.0 (10). To ascertain whether a similar pH threshold existed for disassembly in the H_3PO_4 system, EtxB was subjected to acid treatment for up to 18 h in the pH range of 1.6–3.0 in 0.1 M H_3PO_4 . When the samples were analyzed by SDS–PAGE, a pH threshold of pH 2.2 was observed for pentameric disassembly in the H_3PO_4 system (data not shown), slightly higher than that found in HCl.

The kinetics of disassembly at ambient temperature in 0.1 M H_3PO_4 at both pH 1.7 and pH 1.8 were examined by densitometry of SDS–PAGE gels. Pentamer disassembly was observed to follow an apparent first-order process and to occur more rapidly at the lower pH. The rate constants for disassembly were determined to be $0.156 \pm 0.010 \text{ min}^{-1}$ at pH 1.7 and $0.081 \pm 0.006 \text{ min}^{-1}$ at pH 1.8 (Figure 2A,B and Table 1). These kinetic parameters for disassembly could be estimated independently by G_{M1} -ELISA (Figure 2C,D). Again disassembly appeared to follow a first-order process with a rate constant at pH 1.7 of $0.178 \pm 0.021 \text{ min}^{-1}$ ($r^2 = 0.985$) and at pH 1.8 of $0.117 \pm 0.015 \text{ min}^{-1}$ ($r^2 = 0.991$).

Unfolding/disassembly can also be monitored by fluorescence; previous fluorescence analyses of disassembly in the

Table 1: Summary of the Rate Constants for Disassembly of EtxB in Phosphoric Acid^a

technique	pH 1.7		pH 1.8	
	rate constant (min ⁻¹)	half-time (min)	rate constant (min ⁻¹)	half-time (min)
fluorescence	0.192 ± 0.009	3.6	0.090 ± 0.009	7.7
G _{m1} -ELISA	0.178 ± 0.021	3.9	0.117 ± 0.015	6.0
gel densitometry	0.156 ± 0.010	4.4	0.081 ± 0.006	8.6

^a Samples monitored by intrinsic fluorescence and G_{m1}-ELISA were disassembled at 20 °C; samples for gel densitometry analyses were disassembled at ambient temperature. The fluorescence-derived rate constants shown are for phase 1 of a sequential first-order process.

KCl–HCl system at pH values of 1.9 and below indicated a single step process that followed first-order kinetics with the rate constant for disassembly proportional to the square of the H⁺ ion concentration, consistent with the requirement to disrupt two interfaces in the cyclic pentamer simultaneously (10). To identify any differences in disassembly behavior between the two systems, this fluorescence experiment was repeated in H₃PO₄. Changes in the fluorescence intensity were observed from pH 1.9 and below, as in the KCl–HCl system, with no changes apparent at pH 3.0 (Figure 3A). Examination of the residuals revealed, however, that contrary to the single event in the KCl–HCl system, denaturation occurred in a biphasic manner (Figure 3B,C). At pH 1.85 and below, the line of best fit was to a sequential first-order process with an initial rapid phase ($t_{1/2}$ = 2–9 min) followed by a relatively slower phase ($t_{1/2}$ = 10–16 min). A plot of the rate constants for the initial rapid phase against the square of the H⁺ ion concentration showed linear

dependence (r^2 = 0.988) with an apparent first-order rate constant of zero at pH 2.07 (Figure 3D). This is close to the pH value of 1.92 previously reported for zero disassembly of EtxB in KCl–HCl at 20 °C (10). In contrast, the rate for the second slower phase did not show clear pH or H⁺ concentration dependence (data not shown). The average amplitude changes associated with phase 1 and phase 2 over the pH range 1.6–1.85 were 13.7% ± 3% and 24.0% ± 1.3% of the initial signal, respectively.

The rate constant for the first process observed by fluorescence for H₃PO₄ disassembly at 20 °C is in close agreement with those resulting from SDS–PAGE gel densitometry and from G_{m1}-ELISA (Table 1). This indicates that the rapid phase detected by fluorescence is initial disassembly of the pentameric complex (as previously described for the KCl–HCl system) while the slower step is a conformational change in the resulting monomeric species.

Reassembly from Phosphoric Acid. Reassembly was initiated after 1 h in disassembly conditions, and the kinetics of reassembly at pH 7.5 and 20 °C were apparently first-order with a rate constant of 0.098 ± 0.018 min⁻¹ when determined by G_{m1}-ELISA, ($t_{1/2}$ = 7.1 min; Figure 4A) and a rate constant of 0.089 ± 0.005 min⁻¹ by densitometry of SDS–PAGE gels (data not shown). Pentamer reassembly was essentially complete after 30 min in neutralizing buffer with a yield of around 60%. In contrast, pentamer reassembly from the KCl–HCl system at pH 1.7 and 25 °C, when analyzed by G_{m1}-ELISA, was essentially complete 10 min after neutralization with a final yield of only 20% and a rate constant of 0.251 ± 0.015 min⁻¹ ($t_{1/2}$ = 2.8 min; comparable with that reported previously, 12).

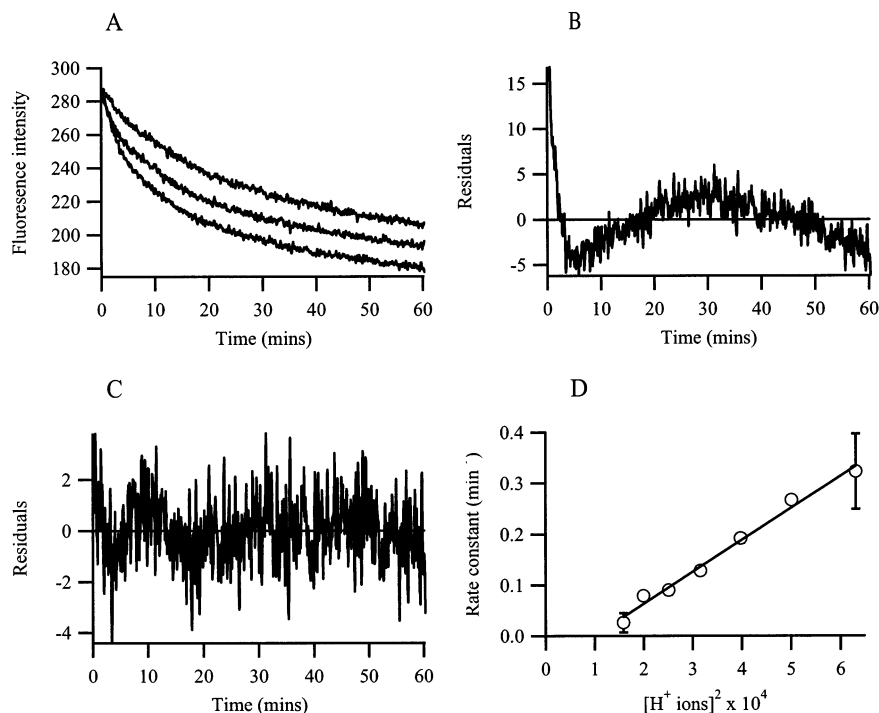


FIGURE 3: Fluorescence analysis of unfolding/disassembly of EtxB in phosphoric acid. Panel A shows time-dependent changes in fluorescence intensity for the acid-mediated disassembly of EtxB at 20 °C in the pH range 1.6–1.8 (excitation 280 nm, emission 350 nm). From top to bottom, the traces are disassembly at pH 1.8, 1.7, and 1.6. From pH 1.6–1.85, the line of best fit was to a two-step first-order process (r^2 = 0.996–0.999). The results displayed are representative of three separate experiments. Panels B and C show residuals from the line of best fit for a single-exponential fit (B) and a double-exponential fit (C) for the time-dependent changes in fluorescence intensity for acid-mediated disassembly at 20 °C, pH 1.6. Panel D shows the linear dependence of the rate constant for acid-mediated disassembly of EtxB on the square of the H⁺ ion concentration (r^2 = 0.988). The rate constants plotted are those determined by changes in intrinsic fluorescence during the first phase of a biphasic process.

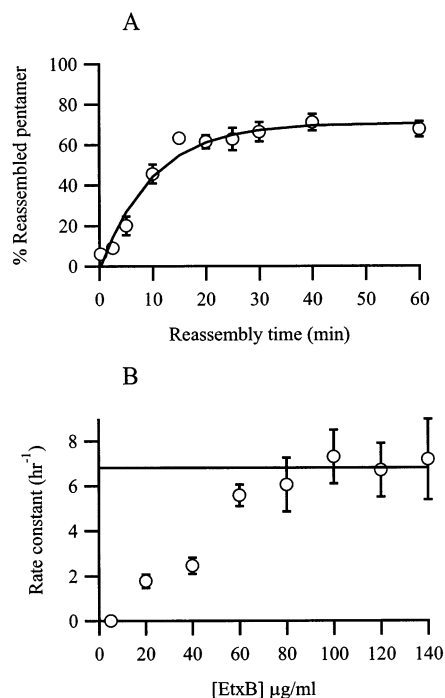


FIGURE 4: Reassembly of EtxB from phosphoric acid. Panel A shows the kinetics of reassembly of EtxB in McIlvaine buffer, pH 7.5, at 20 °C determined by G_{m1} -ELISA ($r^2 = 0.968$). For reassembly, H_3PO_4 -disassembled EtxB was diluted to 100 $\mu\text{g}/\text{mL}$ in McIlvaine neutralizing buffer, pH 7.5, at 20 °C. Samples were removed at selected time points between 0.25 min and 1 h, and the yield of pentamer reassembly was determined. Panel B shows the concentration dependence of pentamer reassembly in McIlvaine buffer, pH 7.5, at 20 °C determined by G_{m1} -ELISA.

The concentration dependence for reassembly from the H_3PO_4 system was analyzed by G_{m1} -ELISA. In the range of 20–140 $\mu\text{g}/\text{mL}$, the yield of pentamer reassembly was independent of concentration and in the region of 60% (data not shown). A plot of the rate constants against concentration showed that the rate of reassembly decreased with decreasing concentrations below 60 $\mu\text{g}/\text{mL}$ but was concentration-independent between 80 and 140 $\mu\text{g}/\text{mL}$ with an average half-time for reassembly of 6.81 ± 0.57 min (Figure 4B). Consistent with this result, reassembly from the KCl–HCl denatured state has been shown to be concentration-independent over the range 50–200 $\mu\text{g}/\text{mL}$ (12). This change of slope (Figure 4B) suggests a multistep process and a change in rate-determining step with concentration; the concentration independence at higher concentrations implies an intramolecular rate-limiting step in these conditions.

In an effort to analyze refolding and reassembly in more detail, we investigated the renaturation process by observing the changes in intrinsic fluorescence (Figure 5A). At all concentrations, plots of the residuals against time showed that the best fit was to a sequential process. Phase 1 of this process was concentration-independent at all concentrations examined. This suggests that phase 1 corresponds to a refolding event (presumably in the monomer) while reassembly to form the pentamer occurs in phase 2. Intrinsic fluorescence could not be used to study reassembly in the KCl–HCl system because most of the time-dependent fluorescent changes occurred during the initial mixing time (data not shown). In H_3PO_4 however, reassembly occurs at a slower rate and the phases can be resolved.

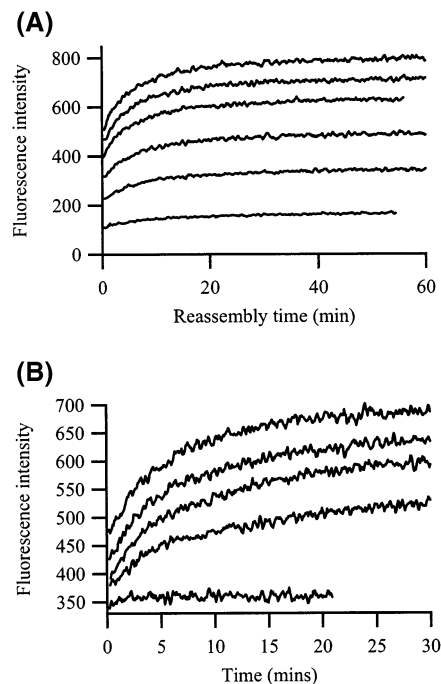


FIGURE 5: Fluorescence analysis of reassembly from phosphoric acid. In panel A, the concentration dependence of reassembly was determined in the range 20–100 $\mu\text{g}/\text{mL}$ over time periods ranging from 55 to 120 min at 20 °C. From top to bottom, the traces are reassembly at 20, 40, 60, 70, 80, and 100 $\mu\text{g}/\text{mL}$. Excitation was at 280 nm and emission at 360 nm with 2.5 nm slit widths. The percent difference in the fluorescence start and end points over the concentration range was $63\% \pm 0.5\%$. Panel B shows the pH dependence of reassembly of EtxB monitored by changes in the intrinsic fluorescence (excitation 280 nm, emission 350 nm). From top to bottom, the traces are reassembly at pH 5.0, 6.0, 6.5, 7.0, and 8.0. EtxB was fully denatured in 0.1 M H_3PO_4 at pH 1.7. The reassembly conditions were at a concentration of 80 $\mu\text{g}/\text{mL}$ at 20 °C in McIlvaine buffer, increasing by 0.25 pH units over the pH range 5.0–8.5. Control was native EtxB at the same concentration of 80 $\mu\text{g}/\text{mL}$.

Reassembly from the KCl–HCl disassembly system has been shown to be pH-dependent with the protonation state of the N-terminus playing a crucial role in the rate of pentamer formation (12), but it could not be determined whether this was an effect on the rate of refolding or reassembly. The pH dependence of refolding and reassembly from H_3PO_4 was investigated by examining the changes in intrinsic fluorescence upon renaturation in the pH range 5.0–8.5. At pH 5.0 over a period of 20 min, no significant change was observed (Figure 5B). However, from pH 6.0 to 8.5, measurable changes were recorded and analyses of the residuals of the spectra over this pH range revealed that at all pH values the line of best fit was to a sequential process. The relevant kinetic parameters have been tabulated for both phases of a sequential process (Table 2) with the first phase, which we attribute to monomer refolding, being pH-independent in contrast to the apparently pH-dependent reassembly phase.

Comparison and Interconversion of Disassembled States. To identify any differences in the conformation of H_3PO_4 and KCl–HCl denatured EtxB, samples were analyzed by far UV circular dichroism (CD). The observed shift to the left in the CD spectrum of EtxB on acidification (Figure 6) is indicative of a loss of ordered secondary structure in the protein, consistent with a significant reduction in β sheet

Table 2: pH-Dependence of Refolding and Reassembly^a

pH	phase 1		phase 2	
	rate constant (min ⁻¹)	half-time (min)	rate constant (min ⁻¹)	half-time (min)
6.00	0.402 ± 0.043	1.7	0.040 ± 0.004	17.7
6.25	0.344 ± 0.044	2.0	0.052 ± 0.004	13.3
6.50	0.538 ± 0.058	1.3	0.073 ± 0.005	9.5
6.75	0.271 ± 0.046	2.6	0.068 ± 0.014	10.3
7.00	0.388 ± 0.042	1.8	0.072 ± 0.006	9.6
7.25	0.637 ± 0.103	1.1	0.106 ± 0.004	6.6
7.5	0.386 ± 0.073	1.8	0.083 ± 0.011	8.4
7.75	0.391 ± 0.068	1.8	0.087 ± 0.009	8.0
8.0	0.507 ± 0.133	1.4	0.125 ± 0.008	5.6
8.5	0.453 ± 0.126	1.5	0.114 ± 0.010	6.1

Fluorescence-derived rate constants were determined for the refolding/reassembly of EtxB over a range of pH values following acid denaturation in 0.1 M H₃PO₄, pH 1.7. The rates have been tabulated for phase 1 and phase 2 of a sequential process. The overall % change in fluorescence was 62% ± 7%.

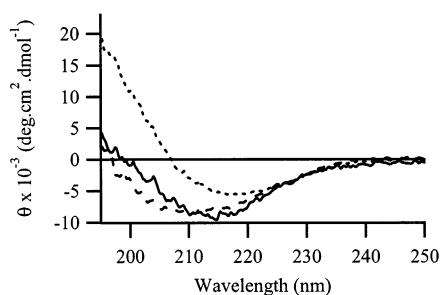


FIGURE 6: Far UV CD spectra. Traces represent native EtxB in McIlvaine buffer, pH 7.5 (dotted line), and following denaturation in KCl–HCl, pH 1.7 (solid line), and in H₃PO₄, pH 1.7 (dashed line).

and an increase in random coil; a similar shift in the spectrum was observed in H₃PO₄ at pH 1.7 as was previously observed in KCl–HCl. However, a significant amount of secondary structure is retained in both cases, and there are apparent differences in the spectra of the KCl–HCl and H₃PO₄ denatured states (Figure 6). These differences must reflect the different effects of the two ionic species on the conformation of the denatured state.

Having demonstrated that H₃PO₄ and KCl–HCl denatured EtxB show differences in their conformation and reassembly competence, we examined the effect of addition of KCl to the H₃PO₄-based denaturing system. When disassembly was carried out in 0.1 M H₃PO₄ at pH 1.7 containing an equimolar amount of KCl, the yield of reassembled pentamer was reduced from 60% to 20%, equivalent to that achieved from the KCl–HCl system (data not shown). If EtxB was initially denatured in H₃PO₄, the loss of reassembly competence upon subsequent addition of KCl was time-dependent and was determined by G_{m1}-ELISA to be an apparently first-order process with a rate constant of 0.327 ± 0.065 min⁻¹ (Figure 7A). This was confirmed by densitometry of SDS–PAGE gels where a similar rate constant of 0.272 ± 0.031 min⁻¹ was obtained (data not shown). This loss of reassembly competence we ascribe to an alteration in the equilibrium between assembly-competent monomers and assembly-defective monomers in the acid-denatured state.

In an effort to identify the process underlying this interconversion, we determined the temperature dependence of the rate constants for the process leading to loss of

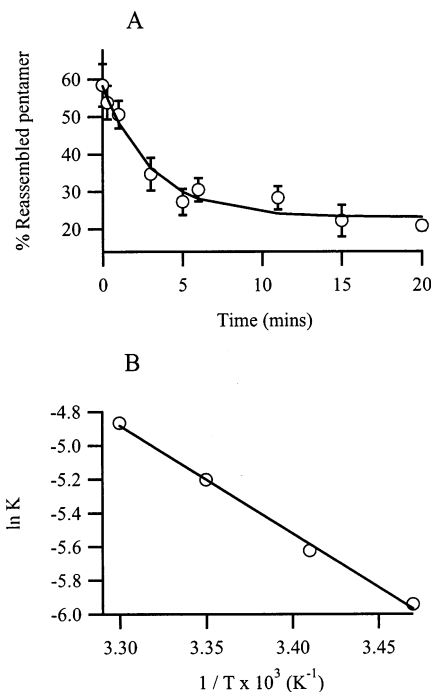


FIGURE 7: Kinetics of the loss of reassembly competence following addition of KCl to EtxB disassembled in phosphoric acid. Panel A shows the G_{m1}-ELISA analyses of the time dependence of the loss of reassembly competence of H₃PO₄-disassembled EtxB in the presence of an equimolar amount of KCl. EtxB was denatured for 1.5 h in H₃PO₄, pH 1.7, at 25 °C. The denatured sample was transferred into 0.1 M H₃PO₄, pH 1.7, containing KCl at a final concentration of 0.1 M and incubated for a further 30 min. At regular time points, aliquots were removed into neutralizing buffer and allowed to reassemble for 1 h. The amount of native pentamer was determined in triplicate by G_{m1}-ELISA, and the rate of loss of reassembly competence was determined. Panel B shows the Arrhenius plot for the loss of reassembly competence of EtxB denatured in H₃PO₄ at pH 1.7 in the presence of equimolar concentrations of KCl–HCl ($r^2 = 0.996$). The rate constants were determined in triplicate by G_{m1}-ELISA.

reassembly competence on addition of KCl to EtxB fully denatured in 0.1 M H₃PO₄, pH 1.7. An Arrhenius plot of the derived rate constants at 15, 20, 25, and 30 °C showed a linear fit ($r^2 = 0.996$) with an activation energy (E_a) of 53 ± 2 kJ/mol (Figure 7B).

We next examined the KCl concentration dependence of the loss of assembly competence. Incubating H₃PO₄-denatured EtxB in KCl, at concentrations ranging from 0.5 to 5 mM, had no effect on pentameric reassembly, but a loss of reassembly competence was observed at concentrations of KCl from 10 to 200 mM (Figure 8A,B). The percentages of reassembly-competent and -incompetent material in this range can be converted to pseudo-equilibrium constants using the equation

$$\text{pseudo-}K_{\text{eqi}} = \frac{\% \text{ reassembly-competent EtxB}}{\% \text{ reassembly-incompetent EtxB}}$$

The natural log of the equilibrium constants when plotted against the concentrations of KCl showed a linear fit (Figure 8C). Because K can be related to ΔG by the expression $\Delta G = -RT \ln K$, the value of effect of KCl on ΔG can be calculated to be 55.4 kJ/mol/M.

Other Denaturation Systems. Since the reassembly yield of EtxB is clearly dependent on the ions present in the

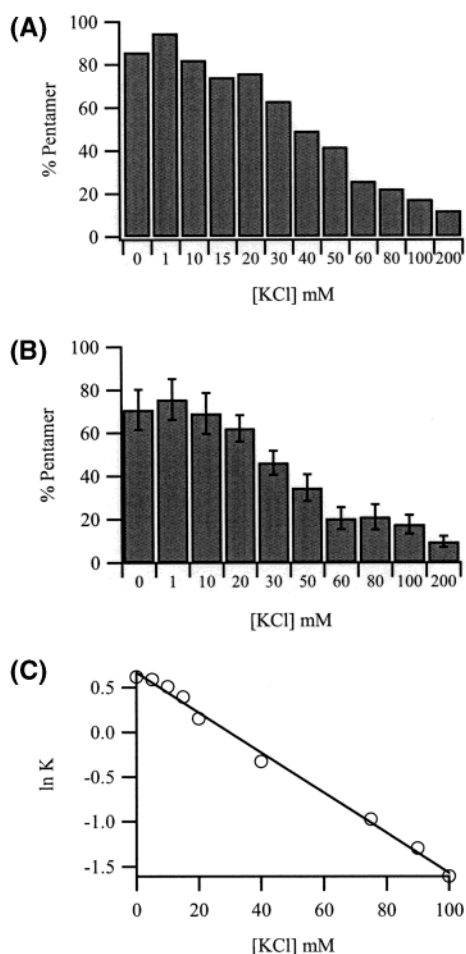


FIGURE 8: Loss of reassembly competence of H_3PO_4 -disassembled EtxB in the presence of increasing amounts of KCl. H_3PO_4 -disassembled samples were incubated for 1 h in the presence of various concentrations of KCl (1–200 mM) prior to reassembly in McIlvaine buffer, pH 7.5, at 25 °C. The results were analyzed (A) by gel densitometry and (B) in triplicate by G_{m1} -ELISA. Panel C presents a plot of the natural log of pseudo- K against [KCl] in the range 0.005–0.1 M.

denaturation buffer during acid denaturation, we examined other denaturation systems in more detail.

First, the effects of using a minimal ionic strength acid denaturation system were examined. Reassembly of native pentamers following low ionic strength HCl denaturation in the absence of salts was ~80% (Figure 9A), equivalent to the maximal reassembly observed in “double-jump” experiments. Addition of salts to the HCl-denatured protein resulted in a concentration- and time-dependent loss of assembly competence that was dependent on the salt used. The shift toward assembly incompetence was studied in a range of sodium salts and in a range of chloride salts and was found to be highly dependent on the anion species but much less so on the cation, the order of the effect being $\text{Na}_2\text{SO}_4 \gg \text{NaI} > \text{CaCl}_2 > \text{KCl} \approx \text{NaCl}$ (data not shown). The addition of only 10 mM Na_2SO_4 to the disassembly mix reduced reassembly from 80% to 20%. In all systems tested, the minimal yield of reassembly at higher ionic strength was 15%–30%. No correlation was observed with the nature of the salt used, for example, the effects did not follow the Hofmeister series.

Second, the use of the widely used chemical protein denaturant guanidinium chloride (GdmCl) was examined.

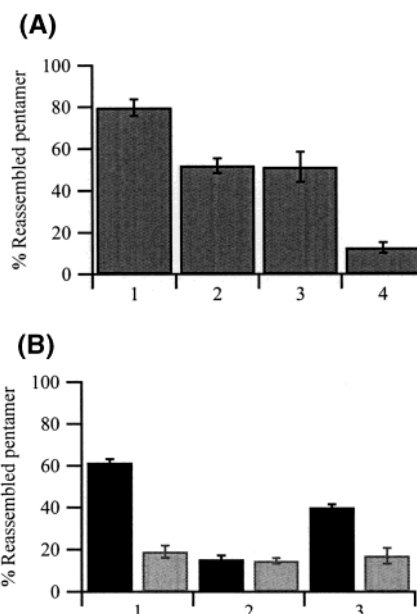


FIGURE 9: Variation in the percentage of reassembly-competent monomers following denaturation in the GdmCl, KCl–HCl, and H_3PO_4 systems as analyzed by G_{m1} -ELISA: (A) yields of native pentamer after reassembly from HCl (sample 1), GdmCl (sample 2), H_3PO_4 (sample 3), and KCl–HCl (sample 4); (B) inhibition of reassembly of EtxB after denaturation in H_3PO_4 and KCl–HCl upon addition of 0.5 M GdmCl. EtxB was fully disassembled in H_3PO_4 (black) or KCl–HCl (grey), pH 1.7, for 2 h. To each sample, GdmCl was added to a final concentration of 0.5 M, and each sample was divided into two aliquots. One aliquot was immediately neutralized (sample 2). The second aliquot was incubated for 2 h prior to neutralization (sample 3). Sample 1 is the control.

The optimum conditions for reversible GdmCl disassembly were first established. Remarkably, in the presence of 5 M GdmCl, temperatures in excess of 60 °C were required to disassemble EtxB from its pentameric state. Both G_{m1} -ELISA and SDS-PAGE analyses confirmed that reassembly yields in excess of 50% were obtained from GdmCl-denatured EtxB (Figure 9A).

We then investigated the effects of the addition of GdmCl to KCl–HCl- and H_3PO_4 -denatured material. GdmCl was added to both H_3PO_4 - and KCl–HCl-denatured EtxB at a concentration of 0.5 M, which would not in itself result in denaturation. Addition was either at the start of the disassembly process or at the neutralization step. The results revealed that the presence of 0.5 M GdmCl inhibited reassembly of both KCl–HCl- and H_3PO_4 -denatured EtxB (Figure 9B). However, the presence of GdmCl during denaturation resulted in a greater effect than when it was present only during reassembly. Hence inclusion of GdmCl in the disassembly process has a direct negative effect on the assembly competence of the monomers with the yield of native pentamer reverting close to the 20% obtained from the KCl–HCl system.

DISCUSSION

An Efficient Denaturation/Renaturation System for EtxB Pentamer. Because the biological properties of proteins arise primarily from their native conformations considerably more attention has been focused on the native conformation than on the denatured or unfolded state. However, the denatured state plays an important role in determining folding pathways

and stability, and the characterization of the conformational properties of the denatured state is an important step in developing an understanding of how a protein folds. The properties of the denatured states of proteins are dependent on the solvent conditions, and proteins may adopt at least three different states, that is, the native state, the unfolded state, or a compact molten globule denatured state (16). Furthermore, the persistence of large amounts of residual structure has been demonstrated in "denatured" proteins, especially in the presence of salts (reviewed in ref 17). The residual structure of many denatured proteins has been found to have little effect on the rates of refolding, and a number of reports have shown similar refolding kinetics for proteins denatured in acid, urea, and GdmCl. Acid- and GdmCl-denatured ribonuclease A (18), lysozyme (19), and α -lactalbumin (20) have all shown the same rate-limiting kinetic events, and identical refolding kinetics are reported for acid- and urea-unfolded staphylococcal nuclease (21) and barnase (22). However, here we demonstrate not only that the denaturation system used has a large impact on the folding kinetics and yield of reassembly of EtxB but also that these effects are subtle and not readily predictable.

The initial aim of our investigations was to identify a denaturation system in which reassembly of EtxB to high yields could be achieved without resorting to "double-jump" experiments. Such a system would allow more detailed elucidation of the refolding and reassembly processes and the potential roles of folding catalysts and molecular chaperones. We have replicated the previously reported irreversible disassembly of EtxB in KCl–HCl and studied a range of other denaturation conditions so that valid comparisons could be made.

Our results show that denaturation is reversible under a variety of conditions, and we have established the optimum conditions for reversible reassembly after denaturation in H_3PO_4 , pH 1.7. In this system, both unfolding/disassembly and refolding/reassembly are slower than in the KCl–HCl system investigated previously. As a result, it has been possible, using fluorescence, to resolve the processes of unfolding and disassembly and conversely of monomer folding and pentamer assembly and to demonstrate that pentamer reassembly from H_3PO_4 occurs during the second phase of a sequential process with the initial rapid phase corresponding to the refolding of monomers. The refolding process is pH-independent and concentration-independent, while the reverse is true for the reassembly process. It is likely that the similar pH dependence for refolding/reassembly from the KCl–HCl system also arises from the reassembly step. This pH-dependence was attributed to the protonation state of the N-terminal amino group (12).

The Structural Basis of Reassembly-Competent and -Incompetent Denatured States. The proportion of reassembly-competent material is, however, dependent on the type and concentration of the salts used during the denaturation process, that is, prior to neutralization treatment. A 3-fold increase in the yield of reassembled pentamer has been observed here using H_3PO_4 as the denaturant in place of the previously reported KCl–HCl system, and we have demonstrated that the high reassembly yields of native pentamer from H_3PO_4 are sensitive to addition of equimolar concentrations of KCl prior to renaturation. In this case, reassembly competence decreases with first-order kinetics to the 20%

routinely observed with the KCl–HCl system. Hence the reassembly-competent and reassembly-incompetent states are readily interconvertible in acid denaturing conditions, but the position of the equilibrium is dependent on the ionic species present. The competent species is favored in the presence of HCl or H_3PO_4 , while addition of KCl, other salts, or guanidinium chloride shifts the equilibrium to favor the reassembly-incompetent species.

We previously proposed that the time-dependent conversion of denatured EtxB in KCl–HCl to a reassembly-incompetent state corresponded to a cis/trans isomerization of a peptide bond, presumably the conversion of the native cis bond of Pro93 to the more favored trans configuration in the unfolded state. This hypothesis is consistent with the results observed here. CD spectra suggest that there are differences in conformation between predominantly reassembly-competent denatured material (in phosphoric acid) and predominantly reassembly-incompetent material (in KCl–HCl). Interconversion between the states has properties consistent with cis/trans isomerization in that it is only observed in extreme acid conditions and has a high activation energy. Previous studies have shown the loss of reassembly competence in acid during prolonged KCl–HCl incubations to have an E_a of 76 kJ/mol (12). An E_a of around 80 kJ/mol has been reported for peptide processes that are limited by proline isomerization (23, 24). The value of 53 kJ/mol observed here for the conversion of reassembly-competent to -incompetent on addition of KCl to H_3PO_4 -denatured material falls below these values. However, the activation energy for cis/trans isomerization is dependent on the local conformation around the site of isomerization (25–27). Furthermore, no other reversible process in the acid-denatured state can provide a more plausible explanation for the phenomena observed in this work than prolyl cis/trans isomerization.

It appears that denaturation in most conditions results in the establishment of a cis/trans equilibrium ratio of around 0.2:0.8, that is, favoring the trans conformer. This distribution has frequently been observed for cis/trans equilibria in proline-containing oligopeptides (23). Upon renaturation of EtxB, both isomers undergo an extremely rapid conformational change retaining their respective cis and trans conformations as depicted in Figure 1. Isomerization between these two refolded states does not occur in renaturing neutral conditions within a reasonably measurable period. As a result, only the 20% of monomers retaining the native cis conformation can assemble into native pentamers. The R_{trans} conformers, which in this system constitute 80% of the denatured molecules, are effectively assembly-incompetent.

Renaturation from the H_3PO_4 system occurs by the same pathways, but these conditions in the acid disassembled state shift the $U_{\text{cis}}/U_{\text{trans}}$ equilibrium in favor of the cis conformer with a ratio of 0.6:0.4 and hence increase the yield of native pentamer to 60%. This is in contrast to the ratio of 0.2:0.8, which is observed not only in KCl–HCl but also when the equilibrium is perturbed by the addition of other salts to H_3PO_4 -denatured material. In the absence of KCl, HCl appears to favor the cis conformer with a ratio of 0.8:0.2. Since it is very difficult to characterize interconverting unfolded states, we have not investigated the structural basis or specificity of these ionic effects, but the thermodynamic parameters we have derived for the KCl concentration-

dependent interconversion between the two forms are consistent with cis/trans interconversion. A more detailed analysis of this question is beyond the scope of this paper, which has concentrated on developing a suitable system in which the refolding and reassembly of acid-denatured EtxB can be characterized in kinetic and mechanistic terms.

ACKNOWLEDGMENT

We thank Helen Webb and Wellae Williams for the supply of purified EtxB, Kevin Howland for assistance with CD analyses, and Peter Klappa for valuable discussions.

REFERENCES

1. Minke, W. E., Roach, C., Hol, W. G., and Verlinde, C. L. (1999) Structure-based exploration of the ganglioside GM1 binding site of *Escherichia coli* heat-labile enterotoxin and cholera toxin for the discovery of receptor antagonists, *Biochemistry* 38, 5684–5692.
2. Hirst, T. R. (1995) Biogenesis of cholera toxin and related oligomeric enterotoxins, in *Bacterial Toxins and Virulence Factors in Disease, Vol 8 Handbook of natural toxins* (Moss, J., Iglewski, B., Vaughan, M., and Tu, A. T., Eds) pp 123–184, Marcel Dekker, New York.
3. Spangler, B. D. (1992) Structure and function of cholera toxin and the related *Escherichia coli* heat-labile enterotoxin, *Microbiol. Rev.* 56, 623–647.
4. Merritt, E. A., and Hol, W. G. J. (1995) AB5 toxins, *Curr. Opin. Struct. Biol.* 5, 165–171.
5. Sixma, T. K., Kalk, K. H., Van Zanten, B. A., Dauter, Z., Kingma, J., Witholt, B., and Hol, W. G. (1993) Refined structure of *E. coli* heat labile enterotoxin, a close relative of cholera toxin, *J. Mol. Biol.* 230, 890–918.
6. Sixma, T. K., Pronk, S. E., Kalk, K. H., Wartna, E. S., van Zanten, B. A. M., Witholt, B., and Hol, W. G. J. (1991) Crystal structure of cholera toxin-related heat-labile enterotoxin from *E. coli*, *Nature* 351, 371–378.
7. Jaenicke, R. (1987) Folding and association of proteins, *Prog. Biophys. Mol. Biol.* 49, 117–237.
8. Freedman, R. B. (1992) Protein Folding in the Cell, in *Protein Folding* (Creighton, T. E., Ed.) pp 455–539, W. H. Freeman & Co, New York.
9. Hardy, S. J., Holmgren, J., Johansson, S., Sanchez, J., and Hirst, T. R. (1988) Coordinated assembly of multisubunit proteins: oligomerisation of bacterial enterotoxins *in vivo* and *in vitro*, *Proc. Natl. Acad. Sci. U.S.A.* 85, 7109–7113.
10. Ruddock, L. W., Ruston, S. P., Kelly, S. M., Price, N. C., Freedman, R. B., and Hirst, T. R. (1995) Kinetics of acid-mediated disassembly of the B subunit pentamer of *Escherichia coli* heat-labile enterotoxin. Molecular basis of pH stability, *J. Biol. Chem.* 270, 29953–29958.
11. Ruddock, L. W., Webb, H. M., Ruston, S. P., Cheesman, C., Freedman, R. B., and Hirst, T. R. (1996) A pH dependent conformational change in the B-subunit pentamer of *Escherichia coli* heat-labile enterotoxin: structural basis and possible functional role for a conserved feature of the AB5 toxin family, *Biochemistry* 35, 16069–16076.
12. Ruddock, L. W., Coen, J. J. F., Cheesman, C., Freedman, R. B., and Hirst, T. R. (1996) Assembly of the B subunit pentamer of *Escherichia coli* heat-labile enterotoxin. Kinetics and molecular basis of rate-limiting steps *in vitro*, *J. Biol. Chem.* 271, 19118–19123.
13. Leece, R., and Hirst, T. R. (1992) Expression of the B subunit of *Escherichia coli* heat-labile enterotoxin in a marine *Vibrio* and in a mutant that is pleiotropically defective in the secretion of extracellular proteins, *J. Gen. Microbiol.* 138, 719–724.
14. Amin, T., and Hirst, T. R. (1994) Purification of the B-subunit oligomer of *Escherichia coli* heat-labile enterotoxin by heterologous expression and secretion in a marine *vibrio*, *Protein Expression Purif.* 5, 198–204.
15. Sandkvist, M., Hirst, T. R., and Bagdasarian, M. (1990) Minimal deletion of amino acids from the carboxyl terminus of the B subunit of heat-labile enterotoxin causes defects in its assembly and release from the cytoplasmic membrane of *Escherichia coli*, *J. Biol. Chem.* 265, 15239–15244.
16. Kuwajima, K., Mitani, M., and Sugai, S. (1989) Characterisation of the critical state in protein folding. Effects of guanidine hydrochloride and specific Ca²⁺ binding on the folding kinetics of alpha-lactalbumin, *J. Mol. Biol.* 206, 547–561.
17. Dill, K. A., and Shortle, D. (1996) The denatured state (the other half of the folding equation) and its role in protein stability, *FASEB J.* 10, 27–34.
18. Garel, J. R., Nall, B. T., and Baldwin, R. L. (1976) Guanidine-unfolded state of ribonuclease A contains both fast and slow-refolding species, *Proc. Natl. Acad. Sci. U.S.A.* 73, 1853–1857.
19. Kato, S., Okamura, M., Shinamoto, N., and Utiyama, H. (1981) Spectral evidence for a rapidly formed structural intermediate in the refolding kinetics of hen egg white lysozyme, *Biochemistry* 20, 1080–1085.
20. Kuwajima, K., Hiraoka, Y., Ikeguchi, M., and Sugai, S. (1985) Comparison of the transient folding intermediates in lysozyme and alpha-lactalbumin, *Biochemistry* 24, 874–881.
21. Sugawara, T., Kuwajima, K., and Sugai, S. (1991) Folding of staphylococcal nuclease A studied by equilibrium and kinetic circular dichroism spectra, *Biochemistry* 30, 2698–2706.
22. Matouschek, A., Serrano, L., and Fersht, A. R. (1992) The folding of an enzyme. Structure of the transition state for unfolding of barnase analysed by a protein engineering procedure, *J. Mol. Biol.* 224, 805–818.
23. Brandts, J. F., Halvorson, H. R., and Brennan, M. (1975) Consideration of the possibility that the slow step in protein denaturation reactions is due to cis–trans isomerism of proline residues, *Biochemistry* 14, 4953–4963.
24. Schmid, F. X., Mayr, L. M., Mucke, M., and Schönbrunner, E. R. (1993) Prolyl isomerases role in protein folding, *Adv. Prot. Chem.* 44, 25–66.
25. Tan, Y.-J., Oliveberg, M., Otzen, D. E., and Fersht, A. R. (1997) The rate of isomerisation of peptidyl proline bonds as a probe for interactions in the physiological denatured state of chymotrypsin inhibitor 2, *J. Mol. Biol.* 269, 611–622.
26. Reimer, U., Scherer, G., Drewello, M., Kruber, S., Schutkowski, M., and Fischer, G. (1998) Side-chain effects on peptidyl-prolyl *cis/trans* isomerisation, *J. Mol. Biol.* 279, 4449–460.
27. Jabs, A., Weiss, M. S., and Hilgenfeld, R. (1999) Non-proline *cis* peptide bonds in proteins, *J. Mol. Biol.* 286, 291–304.

BI0354987